

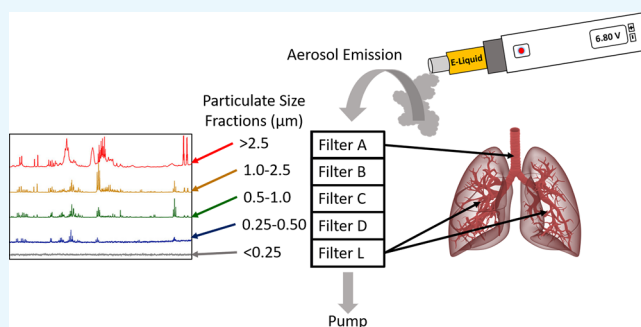
Influence of the E-Cigarette Emission Profile by the Ratio of Glycerol to Propylene Glycol in E-Liquid Composition

Beng G. Ooi,^{*,†} Dibyendu Dutta,^{‡,§} Kavya Kazipeta,^{†,||} and Ngee S. Chong^{*,†,||}

[†]Department of Chemistry, Middle Tennessee State University, P.O. Box 68, Murfreesboro, Tennessee 37132, United States

[‡]Department of Professional Science, Middle Tennessee State University, P.O. Box 83, Murfreesboro, Tennessee 37132, United States

ABSTRACT: The use of electronic cigarettes (E-cig) is popular because of the perception that they are less addictive and safer compared to the traditional cigarettes. Nevertheless, there are still harmful effects associated with chemicals emitted from E-cig. Identifying the sources of the emitted compounds can be challenging because of the differences in the design of E-cig devices and the variability in the composition of E-cig liquids used in these devices. In this study, the emission profiles from impurity-free E-liquids containing only propylene glycol and glycerol in various percentage ratios along with two commercially available E-liquids were evaluated using gas chromatography–mass spectrometry (GC–MS). This study approach allows the elucidation of the transformation pathways of the major emitted compounds without the confounding effects of existing impurities or flavor ingredients added to E-liquids. Analysis of the vapor phases of E-cig emissions detected toxicants such as acetaldehyde, acrolein, benzaldehyde, as well as benzene, toluene, ethylbenzene, and xylene (BTEX) compounds. The amount of glycerol in the E-liquids has a major effect on the concentration of these hazardous compounds emitted because the concentration of these chemicals increased with increasing glycerol percentage in the E-liquid. Acetaldehyde and acrolein increased by 175-fold and 28-fold, respectively, when the glycerol composition was increased from 0 to 80%. Benzaldehyde, naphthalene, diphenyl ether, and glycerol along with menthol and nicotine that were present in the commercial E-liquids were also detected in the aerosol condensates. The cascade impactor data on the distribution of the nicotine and menthol in different size fractions from >2.5 to <2.5 μm allow the estimates of the extent of toxicant deposition in different parts of the pulmonary system including the oropharynx region, the trachea as well as inside the alveoli and bronchioles. In summary, users of E-cig are exposed to harmful chemicals even if the E-liquids contain only propylene glycol and glycerol without flavorings, nicotine, or impurities. Furthermore, this study shows that E-liquids containing higher percentages of glycerol will produce higher levels of toxicants compared to E-liquids with similar percentages of propylene glycol. This finding has important implications to E-cigarette vendors and manufacturers, consumers, and regulatory agencies.



INTRODUCTION

Electronic cigarettes (E-cig) are battery-powered smoking devices that create aerosol containing nicotine and flavoring agents by heating E-liquids. Currently, E-cig is very popular among youth and young adults, with marked increase among middle and high school students.¹ Popularity of E-cig is due to various reasons and perceptions: (1) E-cig is safer compared to conventional cigarettes because E-liquids are composed of different proportions of propylene glycol (PG), glycerol, and flavoring substances that are classified as “Generally Recognized As Safe” (GRAS) by the U.S. Food and Drug Administration, that is, FDA;² (2) E-cig deliver less nicotine and other smoke-related toxins;³ (3) E-liquids come in various flavors that are appealing to the youth;⁴ and (4) E-cig use may aid in cessation of smoking.⁵ Apparently, E-cig use has now become the most commonly used form of tobacco smoking in the U.S., with 3.7%

of adults (approximately 9 million) being regular users of E-cig.⁶

Existing E-cig research data are still relatively less comprehensive compared to that of conventional cigarette smoke in which more than 6500 compounds⁷ with 150 harmful or potentially harmful substances⁸ and more than 50 known carcinogens⁹ have been confirmed. The toxicants produced in the mainstream E-cig vapor include nicotine, glycols, carbonyls, including dicarbonyls and hydroxycarbonyls, volatile organic compounds (VOCs), polycyclic aromatic hydrocarbon, tobacco-specific nitrosamines, and metals.^{10–13} Many of these substances are known toxins, including carcinogens such as formaldehyde and acetaldehyde.¹⁴ The types and concen-

Received: May 22, 2019

Accepted: July 22, 2019

Published: August 5, 2019

trations of chemical constituents produced in the E-cig vapor depend on the formulation and flavor of the E-liquids, and the voltage used.^{14,15}

Toxicants produced from heating the E-liquids are found in the vapor phase, particulate phase, or both. A vast majority of studies investigating the E-cig vapor phase have used gas chromatography coupled with mass spectrometry (GC–MS). In particulate phase analysis, the Harvard compact cascade impactor,¹⁵ the Cambridge filter pads and glass fiber filter pads techniques have been used to collect the total particulate matter for GC–MS analysis.¹⁶ However, the particulate analysis of filter pads does not yield information on the size-dependent distribution of different E-cig particulate phase components. Many studies on the analysis of E-cig vapor constituents are related to investigating the effects of flavoring agents on the formation of E-cig vapor constituents. Because there are thousands of different brands of E-liquids with minor levels of flavor ingredients and various percentages of glycerol and PG, it is nearly impossible to study all of them with regard to their chemical transformation and distribution between the gas and particulate phases. Therefore, it is the goal of this study to probe the E-cig emission profiles based on the ratio of the two major E-liquid components, namely, glycerol and PG, and menthol, one of the most popular E-liquid flavors. This research approach will provide a better understanding of E-cig emission characteristics for many commercially available E-liquid products.

Among the various E-liquid flavors, menthol is one of the most popular flavors, especially among young adults⁴ and women.¹⁷ FDA regulates various flavoring agents such as grape, clove, coffee, and cinnamon in tobacco except for the menthol flavoring. Even though menthol cigarettes are used as a starter product among youths,¹⁸ menthol remains an unregulated tobacco flavoring agent.¹⁹ Thus, it is important to investigate the chemical compounds produced from vaping of E-liquids containing menthol. This study identified the compounds present in the vapor phase of E-cig using Fourier-transform infrared spectrometry (FTIR) and GC–MS. The effects of addition of menthol into the PG and glycerol base composition of E-liquids were studied and compared to the commercial brand of zero nicotine menthol-containing E-liquid. In addition, the total particulate phase of the E-cig vapor was separated by size using a Sioutas cascade impactor followed by GC–MS analysis to determine the concentrations of E-cig vapor constituents in different size-dependent particulate fractions.

RESULTS AND DISCUSSION

Mist Emitted from E-Cigarette. E-liquids are a mixture of PG and glycerol at the various volume percentage ratios of 10:90, 20:80, 50:50, and 80:20 with flavoring additives and may or may not contain nicotine. The visible puff or mist emitted from the E-cig is composed of the vapor and aerosol phases that are distributed and deposited in the respiratory system during inhalation. A previous study has reported the concentration range of 0.161–0.477 mg/m³ for glycerol and 53–175 mg/m³ for PG in the vapor phase of E-cig emission.^{13,20,21} These two major components of E-liquids were found predominantly in the aerosol phase based on the comparison of both the GC–MS data of aerosols collected with the cascade impactor and the vapor phase samples in the Tedlar bags. This is consistent with the low vapor pressures of glycerol and PG due to the strong intermolecular hydrogen bonding interactions within the fine aerosol droplets. The infrared spectral data of E-cig emission

based on their different blend ratios show that PG was found at higher levels than glycerol, even when the PG was present at only 20% in the mixture. Short exposure to PG mist has been reported to cause acute effects on the ocular and pulmonary system.²² Moreover, the PG and glycerol are converted to carcinogenic carbonyl compounds upon heating via the atomizer in the E-cig (Figures 1 and 2).

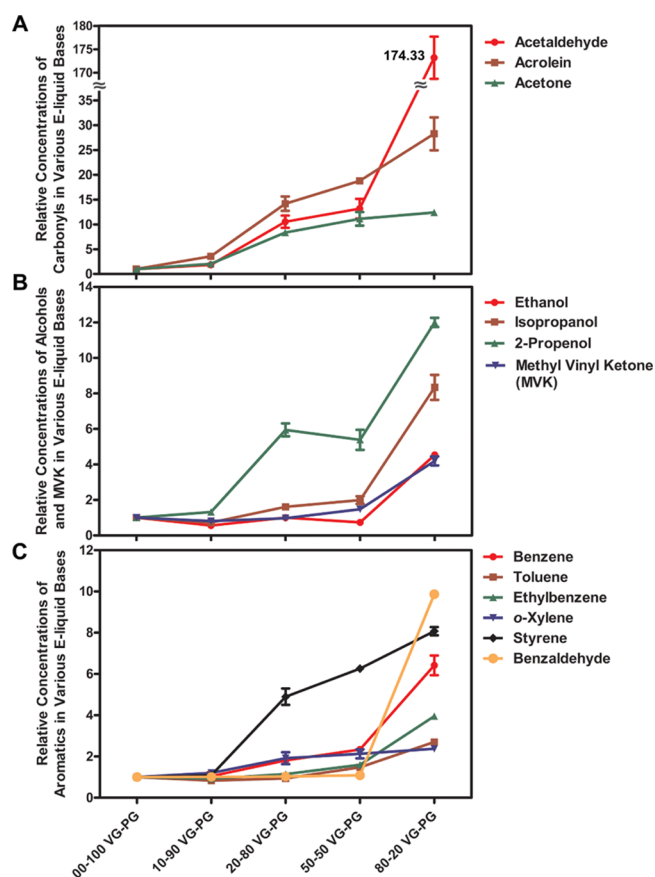


Figure 1. Relative concentrations of emitted VOCs for E-liquids with different percentage ratios of glycerol (VG) and PG. All values were calculated relative to 100% PG. (A) In the plot for carbonyl compounds, the acetaldehyde data point for the VG/PG mixture ratio of 80:20 is plotted with a gap in the scale to accommodate its very high relative level; (B) plot of the relative concentrations of the three alcohols and MVK; (C) plot of the relative concentrations of aromatic compounds.

Analysis of the Vapor Phase Profile by GC–MS. The VOCs observed in GC–MS results of the E-cig mist include mostly compounds with two or three carbon atoms but can also include larger molecular weight compounds like toluene and styrene. The harmful or potentially harmful VOCs include formaldehyde, acetaldehyde, and acrolein, which are some of the toxic carbonyl compounds formed by the thermally assisted reactions of PG and glycerol^{23–25} that are detected in the vapor phase. The analysis of the E-cig vapor phase as a function of the ratio of PG to glycerol in the E-liquids shows that most VOCs were found to be at higher concentrations as the glycerol content in the E-liquid based is increased (Figure 1). Figure 1A shows a 28-fold increase in acrolein concentration as the glycerol is increased from 0 to 80%, which can be explained by the dehydration reaction of the glycerol as shown in Figure 2B. A similar trend was reported by Wang et al.²⁶ that the acrolein

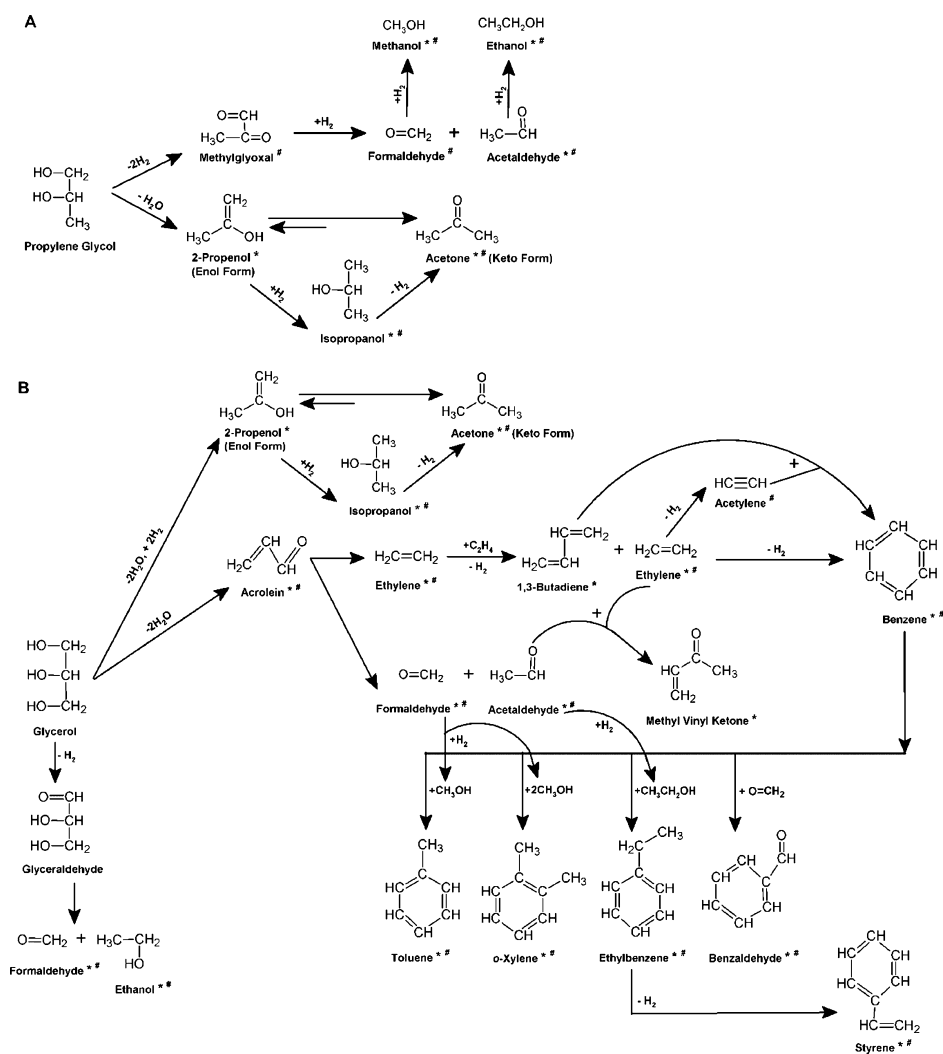


Figure 2. Schematic diagrams showing possible reaction pathways of compounds that are attributed to (A) PG and (B) glycerol. The formation of carbonyl, alcohol, and aromatic compounds as a result of the thermal decomposition of PG and glycerol E-liquid solvents are depicted. The * denote compounds detected in the E-cig emission vapor of this study, and # denote compounds reported by other studies.^{12,14,23,24,38–43}

level increased in the E-cig emission as the E-liquid composition was changed from pure PG to 1:1 VG/PG mixture and finally to pure glycerol at the E-cig temperatures of 270 and 318 °C. An important distinction of this study is that the carbonyl analysis was carried out on the aerosol samples using DNPH derivatization with subsequent liquid chromatography analysis and ultraviolet-diode array detection compared to the current study of the vapor phase analysis of all VOCs using GC–MS over a broader range of VG/PG ratios for the E-liquids. The subsequent reaction of acrolein involves hydrogenation and cleavage to form formaldehyde and ethylene. This glycerol-based pathway for formaldehyde formation is more significant than the PG-based pathway because the experimental data based on extracted ion chromatogram at the m/z value of 30 for GC–MS analysis show that formaldehyde, with molecular mass of 30 amu, was found in the E-cig emissions from E-liquids with 80% glycerol and 20% PG. This important observation underscores the fact that “cloud chasers” who favor the use of E-liquids with a high glycerol composition are at a greater risk of developing adverse health effects due to the higher exposures to acrolein and formaldehyde. Acrolein is considered by the US Environmental Protection Agency²⁷ as a hazardous air pollutant that can cause intense irritation of the

nasal cavity, cytotoxicity in airways, and increased mucus secretion and a risk factor for developing chronic obstructive pulmonary disease.^{28,29}

In fact, many adverse health effects on the respiratory, gastrointestinal, cardiovascular, neurological, and immune systems including exacerbation of pre-existing conditions have been attributed to E-cig, some of which are similar to effects seen with tobacco smoking.^{30–32} According to CDC and NIOSH, the revised immediately dangerous to life or health (IDLH) concentrations for acrolein based on acute inhalation toxicity in human is 2 ppm or 5 mg/m³, whereas for acetaldehyde, the IDLH concentration is 2000 ppm based on data in animals. Although the current study shows that the acrolein concentration emitted for the E-liquid of 80% glycerol and 20% PG is 0.68 mg/m³, which is below the IDLH level, it is above the permissible exposure level (PEL) of OSHA at 0.1 mg/m³. Besides the IDLH and PEL values that are associated with the protection of industrial workers, the lowest observed adverse effect level (LOAEL) can also be used to assess the toxicity of E-cig emission. For acrolein, the LOAEL for inhalation reference dose is 0.9 mg/m³ (0.4 ppm),³³ which is slightly above the measured level at 0.68 mg/m³ for the 80% VG/20% PG E-liquid. The International Agency for Research

on Cancer (IARC) has also classified benzene and formaldehyde as a group 1 or known human carcinogen and acetaldehyde a group 2B or a possible carcinogen for humans.³⁴ For benzene, the estimate of carcinogenic risk from inhalation exposure is in the range of 2.2×10^{-6} to 7.8×10^{-6} for the increase in the lifetime risk of an individual who is exposed for a lifetime to $1 \mu\text{g}/\text{m}^3$ benzene in air.³⁵ Based on the measured benzene concentration of $68 \pm 5 \mu\text{g}/\text{m}^3$ for the E-cig emission of the 80% VG/20% PG E-liquid, the cancer risk is approximately 1 in 10 000.

The GC–MS results on the study of the emissions based on E-liquids with different VG/PG ratios also allow the reaction pathways of the VOCs from the E-cig emissions to be proposed. The expanded and revised schematic diagrams of reaction pathways, compared to those of Bekki and co-workers,²⁴ include additional VOCs generated from PG and glycerol in E-cig emissions that are shown in Figure 2A,B, respectively. The schematic diagrams show reaction pathways consistent with the detection of specific compounds emitted from the E-cig device filled with only the glycerol/PG solvent mixture. As seen in Figures 1 and 2, the E-cig vapor produced from just the base liquid (without any flavoring agent or nicotine) contains, in addition to acrolein, a number of potentially harmful compounds including acetone, benzaldehyde, methacrolein, acetaldehyde, 2-propenol, as well as benzene, toluene, ethylbenzene, and xylene, which are collectively referred to as “BTEX” compounds. Among these detected compounds, the concentration of acetaldehyde increases most significantly by 175-fold as the concentration of glycerol is increased from 0 to 80% in the E-liquid. This implies that the formation of acetaldehyde is greatly influenced by the degradation of glycerol rather than PG. This deduction is consistent with our proposed reaction pathways for PG (Figure 2A) and glycerol (Figure 2B) because the GC–MS data show not only the presence of glycerol-derived acrolein, which is the precursor of acetaldehyde, but also the absence of methylglyoxal, an alternate precursor of acetaldehyde produced via the PG pathway. Although it is inferred that glycerol degradation contributes to elevated levels of formaldehyde and acetaldehyde, it is important to mention that they have been determined to be present in E-liquids at the concentration ranges of 0.114–2.92 $\mu\text{g}/\text{g}$ for formaldehyde and 0.040–10.2 $\mu\text{g}/\text{g}$ for acetaldehyde.³⁶

The presence of both 2-propenol and acetone in the emissions also suggests the occurrence of the tautomerization reaction between the enol and keto forms (Figure 2A,B) with the equilibrium favoring the formation of acetone, which was found at 21–44 times the concentrations of 2-propenol in the vapor phase emissions of E-liquids with the various ratios of glycerol to PG. The 2-propenol and acetone tautomers can also be formed indirectly via the intermediate product of isopropanol for reaction pathways of either PG or glycerol. The similar relative concentration ratios of acetone and 2-propenol (i.e., the comparison of vapors for E-liquids of 80% VG/20% PG to 100% PG) of 12.4 and 11.9, respectively, further corroborate the mechanism for the formation of these two compounds via tautomerization in the reaction pathways for glycerol and PG. As shown in Figure 2A,B, the hydrogenation of formaldehyde and acetaldehyde leads to the formation of methanol and ethanol, respectively. Ethanol is the VOC found at the highest concentration in the emissions of E-cig for various E-liquid formulations. The measured concentrations of ethanol in the vapor phase are highly variable

and dependent on the sampling conditions because ethanol vapor can be absorbed into the aerosol droplets and undergoes a dynamic partition equilibrium between the vapor and aerosol phases. In general, the gaseous ethanol concentration decreases as a function of time as the E-cig mist is cooled to ambient temperature, favoring ethanol condensation and absorption into the aerosol phase or deposition onto the surface inside the Tedlar bag. For the E-liquid of 80% glycerol and 20% PG, the vapor phase concentration of ethanol was determined to be 28.6 mg/m^3 or 15.2 ppm. The measured ethanol concentration would likely be larger if the E-cig device can be interfaced directly to the GC–MS system with cryogenic pre-concentration for immediate analysis of VOCs in the emissions.

Most studies focus on the adverse health effects caused by the flavoring agents and nicotine in the E-liquid, but the root of the problem stems from the formulation of PG and glycerol as solvents or the major components in the E-liquid. Figure 1B shows the increase of the relative concentrations of methanol, ethanol, isopropanol, and methyl vinyl ketone (MVK) as the glycerol percentage increases in the VG/PG mixtures. Both methanol and ethanol were also reported in other prior studies³⁷ as byproducts of the oxidation and thermal decomposition of glycerol in the E-liquid. The very high levels of ethanol in E-cig emissions are of concern because of its intoxicating effect and tendency to affect mental acuity. It is not known to what extent the absorption of ethanol into blood via the inhalation pathway will accentuate the inebriation due to drinking alcohols. MVK was formed via the dehydrogenation reaction of acetaldehyde and ethylene.

The reaction products shown in Figure 2 have relatively high volatility and are easily detected in the vapor phase of E-cig emissions by GC–MS. It is important to note that the schematic diagrams of vapor phase reaction pathways are complementary to those based on E-cig aerosol analysis using the nuclear magnetic resonance technique. A detailed account of the formation of polar compounds found in the aerosol phase has been reported by Jensen et al.³⁸ and Strongin.³⁹ These compounds existing predominantly in the aerosol phase include PG hemiformal, glycerol hemiformal, glycidol, dihydroxyacetone, acetol, acrolein, acetaldehyde, formic acid, and allyl alcohol. The reaction pathways for vapor phase and aerosol phase are intimately connected. For example, acetol or hydroxyacetone can be converted into formaldehyde and acetaldehyde in the glycerol reaction pathway. Likewise, acetaldehyde is converted into acrolein.³⁸

Among the VOCs plotted in Figure 1A–C, the increase in the relative concentrations of aromatic or BTEX compounds emitted is significantly smaller than those of the carbonyl compounds and alcohols. This can be explained by the fact that the reaction pathways for the formation of aromatic hydrocarbons involves more intermediate steps compared to the formation of carbonyls and alcohols. Therefore, the effect of increasing the glycerol percentage 8-fold from 10 to 80% glycerol in the E-liquid mixture was relatively diluted or smaller for affecting the concentrations of the aromatic hydrocarbons or BTEX compounds compared to the alcohols and carbonyl compounds. Benzene is formed by successive reactions of propylene, ethylene, and acetylene to form benzene initially via 1,3-butadiene as an important reaction intermediate. Detailed mechanisms for the formation of benzene from 1,3-butadiene, which was detected in the E-cig emissions for experiments using E-liquids of different VG/PG ratios, have been described previously for experiments based on thermally assisted

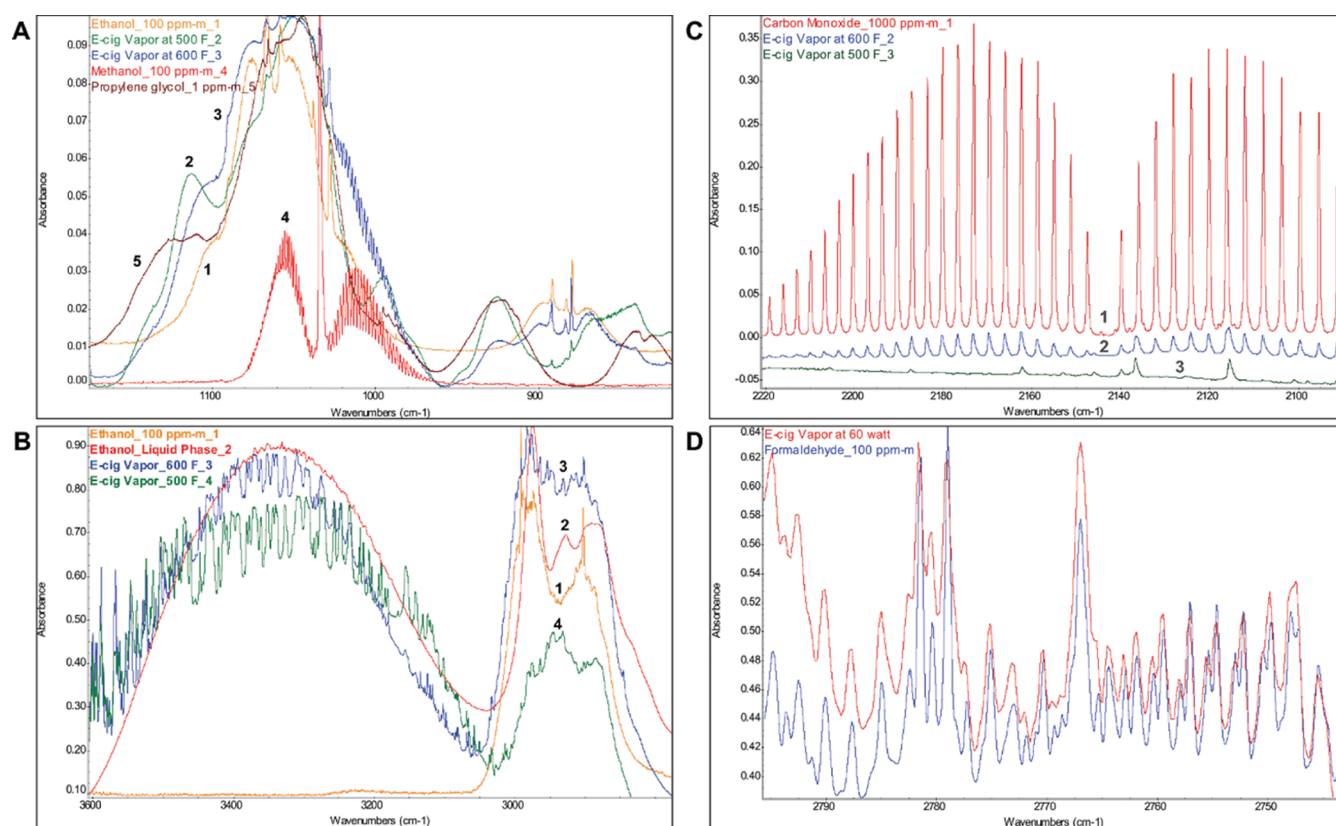


Figure 3. Comparison of FTIR spectra of E-cigarette emissions with reference standards. (A) E-cig vapor spectra at 500 and 600 °F are overlaid with reference spectra of PG, methanol, and ethanol in the fingerprinting region; (B) E-cig vapor spectra at 500 and 600 °F are overlaid with the reference spectra of ethanol in the vapor and liquid phases at the region of 2800–3600 cm^{-1} ; (C) E-cig vapor spectra at 500 and 600 °F are overlaid with the reference spectrum of carbon monoxide in the 2090–2220 cm^{-1} region; (D) E-cig vapor spectrum acquired at E-cig power of 60 W is overlaid with the formaldehyde reference spectrum at 2745–2795 cm^{-1} .

aromatization,⁴⁴ kinetic modeling and reactor experiments under the conditions of 0.15% 1,3-butadiene and 0.4125–3.35% oxygen in nitrogen,⁴⁵ and molecular beam studies of ethynyl radicals and 1,3-butadiene at the collision energy of 45.4 ± 2.1 kJ/mol.⁴⁶ Propylene, ethylene, acetylene, and methane, which play important roles in the formation of benzene and alkyl aromatics, were observed by FTIR or GC–MS in this study, especially at high power settings of E-cig devices when higher concentrations were observed. An alternate pathway for the formation of benzene in E-cig emissions based on the E-liquids containing benzoic acid and benzaldehyde additives was proposed by Pankow et al.⁴⁷ Three benzene formation mechanisms cited include the decarboxylation of benzoic acid, the oxidation and subsequent decarboxylation of benzaldehyde, and the disproportionation of benzaldehyde to form benzyl alcohol and benzoic acid that is decarboxylated to form benzene. The subsequent reactions of benzene with methanol, ethanol, and formaldehyde eventually lead to the formation of toluene and xylenes, ethylbenzene, and benzaldehyde, respectively. Dehydrogenation of ethylbenzene results in the formation of styrene.

Acetaldehyde, acetone, acrolein, ethanol, benzene, toluene, xylene, and styrene that were detected in the vapor phase of this study were also reported in the findings of Herrington and Myers⁴³ using the thermal desorption tube method. Benzaldehyde was detected by GC–MS in both the vapor phase and the different size fractions of aerosol phase collected with Sioutas cascade impactor. Glycerol, PG, and nicotine were detected in the aerosol phase via the GC–MS analysis of cascade impactor

samples. These compounds with high polarity exist primarily in the aerosol phase and tend to condense inside the sample tubings and Tedlar bags. Furthermore, they do not show good recovery via the cryogenically cooled glass bead and Tenax TA traps in the preconcentrator because of their very high enthalpies of vaporization relative to other VOCs. Consequently, they are not observed in the GC–MS analysis and their absence facilitates the analysis of low-level VOCs with similar retention times to these three major constituents of E-cig emissions.

Analysis of the Vapor Phase Profile by FTIR. The GC–MS analysis of E-cig emissions has yielded useful information on the emission profile of VOCs that include C_3 – C_8 hydrocarbons and oxygenated VOCs primarily. The use of GC–MS with a cryogenic pre-concentration technique also allows the quantitative analysis of toxic carbonyl compounds and flavor additives down to the detection limits of 1–10 parts-per-billion by volume (ppbv) in the vapor phase of E-cig emissions. Unfortunately, the GC–MS method suffers from the drawbacks of analyte condensation inside sampling bags or analyte absorption into the aerosol phase prior to sample analysis. Furthermore, GC–MS analysis of small molecules with molecular mass smaller than 35 amu is challenging because of the limitation of the cryogenic pre-concentrator or the background interference of the constituents of air. Hence, the emissions of smaller molecules including CO_2 , CO, methane, ethane, ethylene, methanol, ethanol, and formaldehyde emitted from an E-cig device operated at 500 °F (260 °C) and 600 °F (316 °C) were analyzed by an FTIR spectrometer (Figure 3).

Figure 3A shows the overlay of the infrared reference spectra of ethanol, PG, and methanol with the sample spectra of E-cig emissions at 500 and 600 °F in the fingerprinting region of 800–1200 cm^{-1} . The prominent spectral features of ethanol at the 1080, 1030, and 890 cm^{-1} in Figure 3A and 2955 cm^{-1} in Figure 3B shows that the ethanol signal are easily recognizable by comparing them to those in the reference spectra. The sample spectra in Figure 3B show the existence of ethanol as free gas phase molecules in the C–H stretch band at 3000 cm^{-1} and as the aerosol-bound liquid phase constituent at 3360 cm^{-1} . The reference spectra of ethanol in both gas and liquid phases are overlaid with the sample spectra to corroborate the partition of ethanol in both phases at the E-cig setting of 500 and 600 °F. The liquid phase spectrum of ethanol has the broad hydrogen-bonding O–H band but not the sharp peaks of the C–H stretch band, whereas the gas phase ethanol spectrum shows the opposite description. It is important to note that the O–H vibrational band in Figure 3B is the composite signal of ethanol and other less volatile alcohols including PG and glycerol that exist in the aerosol phase. The C–H band is due to the spectral overlap of ethanol and other VOCs including alcohols like methanol, isopropanol, and 2-propenol that have the C–H covalent bonds.

The average concentrations of ethanol at 500 and 600 °F correspond to the 1236 ± 361 and 3250 ± 449 mg/m^3 , respectively. These concentration values are significantly higher than those measured by GC–MS because the E-cig emissions were generated for immediate analysis by the FTIR method to avoid the condensation of ethanol vapor and its absorption into the aerosol phase which was the case in GC–MS analysis that was performed using samples that were allowed to cool for 30 min in the Tedlar bags after the E-cig vaping. The waiting period allowed the condensation and agglomeration of glycerol and PG in the aerosol particles and therefore prevent their being drawn into the preconcentrator and circumvent the need for the use of excessively high desorption temperature or heating period for the Tenax TA trap and their very intense GC–MS signals that affect the ability to detect or quantify analytes that are at least 100-fold lower in concentrations. The high levels of ethanol can be attributed to the degradation of the E-liquid mixture of glycerol and PG as well as the presence of ethanol as a component of E-liquids. Regardless of whether ethanol is used as a solvent for flavorants or other additives in E-liquids, it is important to determine ethanol concentration because of its inebriating effect or possible conversion into acetaldehyde that can induce adverse health effects. Analysis of ethanol in different E-liquids has been reported by various groups.^{36,43,48} Varlet et al. reported that 30 of the 42 commercial nicotine-containing E-liquids contained ethanol in the range of 6–3675 $\mu\text{g}/\text{g}$.³⁶ Out of 37 nicotine-containing E-liquids analyzed, Poklis et al. reported that two samples contained ethanol concentrations > 100 mg/mL , five samples contained 10–100 mg/mL ethanol, and 17 samples contained 0.05–1.0 mg/mL ethanol.⁴⁸ Therefore, the presence of ethanol in commercial E-liquids could contribute to the ethanol in the gas phase by vaporization. In addition, it is surmised that the thermal degradation of glycerol must have played an important role in producing ethanol because the ethanol vapor concentration, as measured by GC–MS, increased by 4.5-fold for the 80%/20% VG/PG mixture relative to the 0%/100% VG/PG mixture. This suggests that glycerol is capable of further contributing to the thermally assisted production of

ethanol above the level attributed to the volatilization of ethanol as an impurity in the E-liquids.

Figure 3C shows the presence of CO at the level of 7.78 ± 0.06 ppmv or 8.91 ± 0.07 mg/m^3 for the 600 °F emission experiment. This CO value is smaller than the value reported in a recent article that gave the measured CO concentration range of 76.7–2386.9 mg/m^3 for a variety of atomizer filaments, coil configurations, and surface areas at 125 W in sub-Ohm E-cig devices.⁴¹ The CO concentration of 943.7 mg/m^3 or 40 480 ppmv for the 125 W experiment with a nickel coil is also higher than the CO value of 34.6 ± 1.0 ppmv or 39.6 ± 1.1 mg/m^3 for the analysis obtained at E-cig power of 60 W using a Kanthal coil. These CO concentrations in each puff are higher than the National Ambient Air Quality Standard (NAAQS) of CO at 35 ppm for the averaging time period of 1 h. Therefore, it is likely that the indoor level of CO in buildings with no restriction on E-cig puffing may exceed the NAAQS level depending on the setting, the number of vapers, and the puff frequency and duration.

Figure 3D shows the presence of formaldehyde at the level of 22.7 ± 2.9 ppmv or 27.9 ± 3.6 mg/m^3 in the E-cig emission at the maximum power setting of 60 W. The 60 W power setting was used to evaluate the maximum emission exposure of vapers who use the sub-Ohm devices (SODs) at high power levels. Furthermore, the data obtained using the E-cig power of 60 W also allow comparison to a recently published FTIR study of SODs at power levels ranging from 25 to 175 W.⁴¹ According to Misthub.com,⁴⁹ the use of 50 W gives “a nice cool vape with good flavor” and 60 W will yield “massive plumes of vapor with delightful flavor.” For the emission measurement using the temperature setting mode at 600 °F, the formaldehyde concentration was found to be 0.374 ± 0.157 ppmv or 0.459 ± 0.193 mg/m^3 , which is near the detection limit of the FTIR method. At the temperature setting of 500 °F, the formaldehyde level was below the FTIR detection limit. Therefore, the results support previous assertion that as the power setting is increased to achieve a higher vaping temperature, formaldehyde will be formed at higher concentrations.^{50,51} Ogunwale et al. reported the formaldehyde concentration of 8.2–40.4 mg/m^3 based on an E-cig power setting of 9.5 W for 10 puffs with the puff volume of 91 mL.⁵² The decarbonylation reaction of formaldehyde could explain the formation of carbon monoxide according to a previous study of the decomposition of aldehydes on palladium.⁵³ It is possible that similar decomposition could take place on the nickel filament used in the E-cig device because both nickel and palladium are dehydrogenation catalysts that belong to group VIII in the Periodic Table.

Aerosol Profile. The aerosol phase of E-cig was sampled with the Sioutas cascade impactor (SKC Inc. Eighty Four, PA) where a series of five filter stages, designated as the A (inlet end), B, C, D, and L (outlet end), fractionate the aerosol particles according to sizes of >2.5, 1.0–2.5, 0.50–1.00, 0.25–0.50, and <0.25 μm , respectively. Aerosol particles that are larger than the mass median aerodynamic diameter of 10 μm are usually deposited in the oropharynx region of the mouth, particles in the range of 5–10 μm will be deposited in the central airway of the respiratory system, and particles less than 5 μm can reach the bronchioles and alveoli which are considered as the smallest airways in pulmonary system.⁵⁴ However, multiple processes such as aerosol cooling, evaporation/condensation, and coalescence of aerosol droplets can occur in the oral cavity and alter the dynamics of the inhaled aerosol.

This can impact the distribution, deposition, and transfer of the aerosol within the respiratory system.⁵⁵ The main constituents of the E-cig aerosol are polar compounds with minimal volatility that include glycerol and PG. Besides glycerol and PG that are originally in the E-liquids, other compounds like benzaldehyde, diphenyl ether, diethyl phthalate, and naphthalene were detected in the filters from stages A, B, C, and D that fractionate particles ranging from >2.5 to 0.25 – 0.5 μm . The fairly uniform concentrations of these compounds in different filters suggest that they were likely formed via condensation induced by the adiabatic cooling of the aerosols as they experience pressure changes while passing through the narrow slits of the cascade impactor at the pumping speed of 9.0 L/min.⁵⁶ Glycerol and diphenyl ether were also present in the outlet filter L, which fractionates the particulate size fraction of <0.25 μm , suggesting that these components will likely pass through the smallest airways of the respiratory system.

Diethyl phthalate is commonly used as a plasticizer for manufacturing polymer materials. It could have been released via the thermal degradation of plastic components used in the E-cig device. The thermal degradation most likely occurred on the plastic cover attached on top of the heating coil in the atomizer because the heat generated at the coil would accelerate the release of diethyl phthalate or other plastic additives. Naphthalene has previously been reported by Margham et al.⁵⁷ as detectable in E-cig emissions at 5.01 ± 1.2 ng/puff for puffs 1–100 and 5.87 ± 0.84 ng/puff for puffs 101–200, but these levels are statistically indistinguishable from the method blank emissions. A later publication⁵⁸ shows that naphthalene was determined to be present in various E-liquid products at 4.24 – 32.8 ng/mL and quantified as 1.79 – 3.07 ng/mL-puff in the E-cig emissions. The detection of naphthalene, a group 2B or possible human carcinogen, in the cascade impactor analysis of E-cig aerosol emissions shows that naphthalene was produced in vaping because the high purity PG and glycerol used to prepare the E-liquid were analyzed and did not show the presence of naphthalene. Therefore, it will be important to investigate if the formation of naphthalene takes place via the reaction of benzene and either 1,3-butadiene or acetylene.

Diphenyl ether could have resulted from the thermal degradation of polybrominated diphenyl ethers (PBDEs) that is used as a flame retardant coating on plastic materials in the E-cig atomizers and protective casing. Chung and co-workers⁵⁹ reported finding PBDEs in E-cig aerosol and the amounts vary with the brand of E-cig. It is possible that reductive debromination of PBDEs on the metallic heating coil of the E-cig device has resulted in the production of diphenyl ether because it has been reported that iron can catalyze the conversion of BDE-209 or decabrominated diphenyl ether to mono- to tribromo diphenyl ethers.⁶⁰ Except for glycerol, none of the other four aerosol compounds detected on the filters increased in concentration when the ratio of glycerol to propylene glycerol was increased. However, when the glycerol in the E-liquid was increased to 80%, the amount of benzaldehyde in the vapor phase increased sharply by about 10-fold.

Menthol Flavoring and Nicotine. Two commercially available E-liquid products named Hangsen Menthol, one without nicotine and the other with 18 mg nicotine/mL, are plotted as column charts of VOCs emitted from E-cig in Figure 4. Because both Hangsen Menthol products are based on 10% VG/90% PG E-liquid formulation, the variation of their VOC concentrations compared to those of the 10% VG/90% PG E-

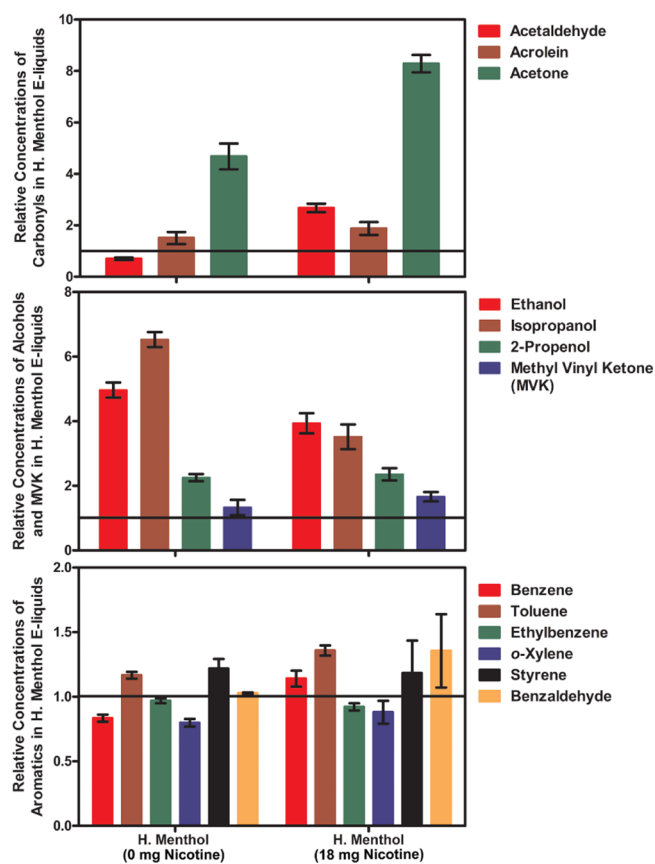


Figure 4. Relative concentrations of VOCs emitted from E-cig using menthol-containing E-liquids with 0 and 18 mg nicotine/mL, respectively. The relative concentration ratios of emitted VOCs were based on the comparison of vapor phase constituents from Hangsen Menthol and the E-liquid base that are 10% VG/90% PG. The horizontal line at 1.0 in the three charts represents the reference level above which the Hangsen Menthol VOCs are increased and below which the VOCs are decreased relative to the E-liquid base. The GC–MS analysis shows the menthol concentrations of 3.70 ± 0.16 and 3.10 ± 0.27 mg/mL for the Hangsen Menthol without and with nicotine, respectively.

liquid base could be attributed to menthol and/or nicotine. Figure 4 shows that the concentrations of acetone, ethanol, and isopropanol are increased about 4-fold (i.e., relative concentrations of greater than 4 on the Y-axis) in the menthol-containing E-liquids compared to the corresponding measurements for the 10% VG/90% PG E-liquid base. For the aromatic compounds, Figure 4 shows that there is not much difference in their concentrations whether the E-liquids contain menthol or nicotine and their relative concentrations are clustered in the narrow range of 0.8–1.3 around the horizontal line at 1.0 and are unaffected by the VG/PG ratio. For acetone, the presence of menthol alone contributed to its 4.7-fold increase, whereas the addition of both menthol and nicotine to the E-liquid contributed to an 8.3-fold increase. Isopropanol was increased 6.5-fold with the addition of menthol alone, but the increase dropped to 3.5-fold for the E-liquid with both menthol and nicotine. Menthol also caused a smaller increase in the amount of 2-propanol in the vapor phase. Acetaldehyde concentration was found to decrease for E-liquid with only menthol to the E-liquid but increased by 2.7-fold for the E-liquid with both menthol and nicotine.

Menthol is detected in the aerosol phase as opposed to the gas phase because of its high boiling point of 214.6 °C and relatively high enthalpy of vaporization of 56.6 kJ/mol. The distribution of menthol in the various size fractions of the aerosol phase was measured by the Sioutas cascade impactor. The menthol distribution in the E-liquid without nicotine is reported as 6% for the A-filter, 5% for the B-filter, 7% for the C-filter, 67% for the D-filter, and 15% for the L-filter. For the E-liquid with 18 mg/mL nicotine, the menthol distribution is similar with values of 7% for the A-filter, 7% for the B-filter, 13% for the C-filter, 57% for the D-filter, and 16% for the L-filter. This distribution shows that a large proportion or 82–85% (i.e., sum of D- and L-filter contribution) of the emitted menthol can permeate as far as the smallest airways based on their small aerosol particle sizes of less than 0.25 μm . According to Yerger,⁶¹ menthol acts as a local anesthetic that can mask the harsh taste of tobacco smoke as well as modulates the effects of nicotine in ways that allow tobacco companies to adjust the delivery of both to maximize nicotine addictive effects. The remaining 18% of the emitted menthol that was retained in A, B, and C filters showed that menthol can be deposited in the mouth and throughout the pulmonary system. Therefore, it presents a soothing effect throughout, masking any unpleasant sensation of vaping and allowing individuals to tolerate long periods of vaping.

Nicotine from a 12-puff sample was deposited in all the filters of the Sioutas cascade impactor. Its percentage distribution is measured as 12% for the A-filter, 11% for the B-filter, 42% for the C-filter, 1% for D-filter, and 34% for L-filter. This distribution shows that nicotine is mostly found in the two size fractions of 0.50–1.0 and <0.25 μm for the C-filter and L-filter, respectively. This means that a large proportion of the nicotine can be deposited in the bronchioles and alveoli. While no nicotine was detected in the zero-nicotine commercial Hangsen Menthol, the nicotine concentration in the Hangsen Menthol E-liquid marked to contain 18 mg/mL nicotine by the manufacturer actually has 20.3 ± 0.52 mg/mL of nicotine. Using the previously published average E-liquid consumption rate of 9.29 ± 0.24 mg/puff⁶² and either the measured or labeled concentrations of E-liquid constituents like nicotine or menthol, one can estimate the mass of a given constituent per puff in a specific aerosol size fraction. Based on the sampling conditions of the Sioutas cascade impactor, one puff of E-cig aerosol emission was found to contain 15.3 μg nicotine and 2.3 μg menthol in the smallest aerosol size fraction of <0.25 μm . Future work on the E-cig aerosol study will need to investigate the role of the airflow rate of E-cig devices. The airflow rate has been shown to modulate the toxicant profiles and the rate of E-liquid consumption.⁶³

E-liquids are generally produced without strict industry guidelines and regulations with regards to amounts of flavorings and nicotine. This 12.8% discrepancy in the nicotine concentration (i.e., measured value of 20.3 mg/mL compared to the labeled value of 18 mg/mL) can be attributed to the E-liquid being manufactured in local facilities where there is a lack of rigorous quality control, sophisticated production equipment, or trained professionals, resulting in the mislabeling of nicotine content in the E-liquids. The accurate labeling of nicotine concentration in cigarette products is of paramount importance because nicotine is a highly addictive and psychoactive compound.⁶⁴ Many users of E-cig rely on the accurate labeling of nicotine content in the E-liquid as a guide in an effort to quit smoking traditional cigarettes. The discrepancy

in labeled and measured nicotine levels in this study further corroborates similar inconsistencies for E-liquids sold in New York,⁶⁵ North Dakota,⁶⁶ and South Korea.⁶⁷

CONCLUSIONS

A number of harmful compounds including formaldehyde, acetaldehyde, methylglyoxal, acrolein, acetone, benzaldehyde, as well as the BTEX compounds were among the components detected in the vapor phase of E-cig. These compounds were produced primarily by the oxidation and thermal decomposition of glycerol and PG, the two components that make up the carrier solvent in the E-liquid. The higher the percentage ratio of glycerol to PG, the higher the concentrations of the carbonyl compounds emitted especially the acetaldehyde, benzaldehyde, acrolein, and acetone. Similarly, the concentrations of the alcohols and BTEX compounds were also increased but to a smaller degree compared to the carbonyl compounds. Benzaldehyde, diphenyl ether, and diethyl phthalate were also detected in the aerosol phases of E-cig containing only the glycerol/PG solvent mixture. Nicotine and menthol in the Hangsen Menthol E-liquid could be deposited in the mouth and throughout the pulmonary system even when passing through the smallest airway of the bronchioles and alveoli at the concentrations of 15.3 and 2.3 $\mu\text{g}/\text{puff}$, respectively. Other components emitted from E-cig that could be deposited in the mouth and airways were glycerol, benzaldehyde, diphenyl ether, diethyl phthalate, and naphthalene. Further study is necessary to investigate if debromination of flame retardants based on PBDEs occurred in the E-cig atomizer and produced a small amount of diphenyl ether. Although E-cig was initially presented as an alternative to tobacco smoking and as a substitute to help smokers quit smoking, there is still a long list of health risks associated with its use.

MATERIALS AND METHODS

Reagents and Chemicals. Two bottles of 30 mL Hangsen Menthol E-liquid (18 mg/mL nicotine and 0 mg/mL nicotine) with a base composition of 10% vegetable glycerin/glycerol (VG) and 90% PG were purchased from [Madvapes.com](#). Glycerol (>99.5%) and PG (99.5%) used in the vapor phase study and particulate measurements using the cascade impactor were purchased from Thermo Fisher Scientific (Waltham, MA) and VWR International (Suwanee, GA), respectively. Other reagents and standards including nicotine, menthol, acrolein, acetone, ethanol, isopropanol, benzaldehyde, benzyl alcohol, acetaldehyde, and methylene chloride, with their purities ranging from 95 to 99.9%, were purchased from either Sigma-Aldrich, St. Louis, MO or Fisher Scientific, Pittsburgh, PA. E-liquids with only the base formulations of 10% glycerol and 90% PG (10:90 VG/PG) similar to the base formulation of Hangsen Menthol was prepared in the laboratory and was used as control. Other E-liquid base compositions such as 100% PG, 20:80 VG/PG, 50:50 VG/PG, and 80:20 VG/PG were prepared in the laboratory. The commercial Hangsen Menthol E-liquids were diluted 10-fold with methanol for GC–MS analysis of the liquid.

Sampling of the Vapor Phase. An Innokin Iclear 30S (Shenzhen, China) E-cig with a 3 mL liquid tank volume, Iclear 30S atomizer coil made of Kanthal (2.80–6.90 V), and Istick 30 W battery with a variable voltage of 2.0–8.0 V was purchased from Smoke & Mirrors House of Vapor, Murfreesboro, TN.

The Innokin E-cig device was used for the collection of both vapor and particulate phase samples from E-liquids with various VG/PG ratios for GC–MS analysis. The E-cig was operated at 4.80 V and vaped at 3 s per puff for a total of 12 puffs. The vapor samples were collected in Tedlar bags (SKC Inc, Eighty Four, PA) that were connected to an inlet port on the inside of the Vac-U-Chamber (SKC Inc, Eighty Four, PA). The same inlet port was also connected via tubing from the outside fitting of the Vac-U-Chamber to the E-cig emissions. The outlet port of the Vac-U-Chamber was connected to a sampling pump with a flowrate of 2.0 L/min, which is a sampling flowrate used previously for the cigarette emission study.¹⁴ Just before sampling, the valve of the Tedlar bag was opened, the lid of the Vac-U-Chamber was closed, and the pump was activated to create a partial vacuum inside the chamber that allowed the E-cig smoke to be drawn into the Tedlar bag. The smoke-filled Tedlar bags were kept undisturbed for at least 1 h to let the aerosol phase deposited inside the bags so that only the vapor fraction of the smoke could be injected into the GC column for analysis.

Sampling of the Particulate Phase. A Sioutas cascade impactor (SKC Inc., Eighty Four, PA) was used to collect the size-dependent particulate fractions of the E-cig emissions. Particles were deposited onto five different filter pads with the size fractions of filter A (>2.5 μm), filter B (1.0–2.5 μm), filter C (0.50–1.0 μm), filter D (0.25–0.5 μm), and filter L (<0.25 μm). The discs of the Sioutas cascade impactor are made of anodized aluminum with O-rings being Buna-N (nitrile) and filter retainers acrylic. A 25 mm diameter SKC PTFE filter with 0.5 μm pore size was placed between discs labeled A, B, C, and D, whereas a 37 mm diameter SKC PTFE filter with 2.0 μm pore size was used for the filter L. For sampling, a constant flow rate of 9.0 L/min was maintained using the Leland Legacy Pump (SKC Inc, Eighty Four, PA). After sampling, the impactor was disassembled in a dust-free environment, and all the filters were placed in individual vials with 5 mL methylene chloride for extraction. The extraction of analytes in the five particulate fractions was done by sonicating the filters for 1 h in an ultrasonic bath (Fisher Scientific, Pittsburgh, PA). The extract volumes were reduced to 1.5 mL by gently blowing nitrogen gas using a 6-position solvent evaporator (Sigma-Aldrich, St. Louis, MO). The concentrated samples were filtered using Phenex 0.2 μm filters (Phenomenex, Torrance, CA) prior to GC–MS analysis.

Sampling and Analysis of Vapor Phase by FTIR Spectrometry. The vapor emissions of the Joyetech eVic-VT E-cig device (www.joyetech.com) with the dual selection modes of variable temperature (200–600 °F) and variable power (1–60 W) were analyzed by FTIR spectrometry. The mist from the E-cig device with a nickel heating coil was transferred via a tubing with a filter pad into a pre-evacuated Tornado 10 m gas cell from Specac (Orpington, England) before being analyzed using a Varian FTS-7000 FTIR spectrometer with a mercury cadmium telluride (MCT/A) detector. Spectra were acquired for 30 scans at a spectrometer resolution of 0.5 cm^{-1} and processed without zero filling and using the Norton-Beer apodization method. The Varian spectral data files were exported to the Thermo OMNIC format for analysis. The infrared spectra of the E-cig vapor phase were compared to infrared reference spectra of carbon monoxide, methanol, ethanol, formaldehyde, and ethylene. These reference infrared spectra for quantitative analysis were downloaded from the Pacific Northwest National Laboratory

website or retrieved from the infrared spectral library of infrared analysis (Anaheim, CA). The absorbance values of the reference IR spectra with known ppm-meter values were compared to those of the sample spectra in order to calculate the analyte concentrations based on Beer's law. Peak areas were generally used for the quantitative analysis of compounds at spectral regions with no spectral interference. In a few cases, the peak heights were used to circumvent the difficulty of the peak area integration due to the partial spectral peak overlap.

GC–MS Analysis of Liquid, Vapor, and Particulate Phases. The vapor phase was analyzed using an Agilent 6890 gas chromatograph (GC) coupled to an Agilent 5973 quadrupole mass spectrometer (MS). A 16-position autosampler for automated sequential mode analysis was connected to the GC–MS via the NUTECH 8900DS preconcentrator. The preconcentrator has three cryogenic traps, the glass bead trap, Tenax TA trap, and the cryofocuser. An accessory called GC Chaser from Zip Scientific (Fast GC Technology, Goffstown, NH) was used to improve the GC oven ventilation during cool-down cycles. The preconcentrator was set to preheat to 10 °C, whereas the cooling temperature was set at –150 °C, the desorption temperature at 20 °C with preheat time 2 s, and desorption flow at 15 mL/min with desorption time 2 min. The GC separation was performed using the Rxi-1ms capillary column (Restek, Bellefonte, PA) with the stationary phase of 100% polydimethylsiloxane and column parameters of 60 m \times 0.32 mm i.d. and a film thickness of 1.00 μm . Initially, the oven was set at 30 °C for 3 min. The GC oven temperature was then programmed to ramp three times sequentially without any hold, from 30 to 100 °C at 5 °C/min, from 100 to 150 °C at 12 °C/min, and finally from 150 to 220 °C at 15 °C/min. The final temperature was held for 4 min. The GC inlet temperature was maintained at 320 °C, and the helium carrier gas flowrate was set at 28 cm/s. A mass spectrometer was operated in the simultaneous full scan, and selected ion monitoring (SIM) modes. The electron impact ionization was operated with electron energy of 70 eV. The interface temperature was set at 320 °C, and mass spectra were recorded in the m/z range of 29–350 amu.

The Shimadzu QP2010S GC–MS was used in a splitless injection mode to analyze 1.0 μL sample extracts from the cascade impactor filters with different size fractions of the aerosol phase in the E-cig emission. The GC column was a Phenomenex ZBS-HT (Bellefonte, PA) polyimide-coated fused silica column 5% phenyl/95% dimethylpolysiloxane 30 m \times 0.25 mm i.d., film thickness 0.25 μm . Initially, the oven was held at 50 °C for 3 min followed by three stages of temperature ramp-up. First, the temperature was increased from 50 to 150 °C at 5 °C/min and held for 1 min, then to 220 °C at 15 °C/min and held for 3 min, and finally to 320 °C at 25 °C/min and held for 5 min. The inlet temperature was maintained at 250 °C, and the flowrate of carrier helium gas was set at 40 cm/s. The mass spectrometer was operated in the scan mode with its GC interface temperature set at 320 °C and the MS ion source temperature kept at 200 °C. Mass spectra were acquired in the mass range of 35–450 amu.

The analytes from the vapor and aerosol phases were identified via mass spectral matching of sample spectra with reference spectra from the NIST 2014 MS database. In cases of ambiguity in spectral matches with compounds having similar match indices, the chemical identity was confirmed by evaluating the degree of fit of the unknown compound on the linear regression plot of the GC retention times and the

corresponding retention indices for a set of compounds analyzed using the same GC method. The concentrations of E-cig smoke constituents were determined using linear regression equations from standard calibration plots based on the linear slope and non-zero intercept. Graphs were prepared using GraphPad Prism V.5 software, and chemical structures were drawn using ACD/ChemSketch V.2 software. Data are reported as “mean \pm 1 standard deviation” for triplicate analysis of samples.

AUTHOR INFORMATION

Corresponding Authors

*E-mail: Beng.Ooi@mtsu.edu (B.G.O.).

*E-mail: Ngee.Chong@mtsu.edu (N.S.C.).

ORCID

Ngee S. Chong: 0000-0002-7845-6492

Present Addresses

§Department of Medicine, New York Medical College, Valhalla, NY 10595.

||Intone Networks Inc., 10 Austin Avenue, Iselin, NJ 08830.

Notes

The authors declare no competing financial interest.

ACKNOWLEDGMENTS

The authors would like to thank the MTSU Graduate Studies and the Department of Chemistry for supporting the research project and providing funds for publication.

REFERENCES

- (1) Aszyk, J.; Kubica, P.; Woźniak, M. K.; Namięśnik, J.; Wasik, A.; Kot-Wasik, A. Evaluation of flavour profiles in e-cigarette refill solutions using gas chromatography–tandem mass spectrometry. *J. Chromatogr. A* **2018**, *1547*, 86–98.
- (2) Kaur, G.; Muthumalage, T.; Rahman, I. Mechanisms of toxicity and biomarkers of flavoring and flavor enhancing chemicals in emerging tobacco and non-tobacco products. *Toxicol. Lett.* **2018**, *288*, 143–155.
- (3) Caponnetto, P.; Campagna, D.; Papale, G.; Russo, C.; Polosa, R. The emerging phenomenon of electronic cigarettes. *Expert Rev. Respir. Med.* **2012**, *6*, 63–74.
- (4) Zare, S.; Nemati, M.; Zheng, Y. A systematic review of consumer preference for e-cigarette attributes: Flavor, nicotine strength, and type. *PLoS One* **2018**, *13*, No. e0194145.
- (5) Etter, J.-F.; Bullen, C. Electronic cigarette: Users profile, utilization, satisfaction and perceived efficacy. *Addiction* **2011**, *106*, 2017–2028.
- (6) Schoenborn, C. A.; Gindi, R. M. Electronic cigarette use among adults: United States, 2014. *NCHS Data Brief* **2015**, *217*, 1–8.
- (7) Rodgman, A.; Perfetti, T. A. *The Chemical Components of Tobacco and Tobacco Smoke*; CRC press: Boca Raton, Florida, 2016.
- (8) Fowles, J.; Dybing, E. Application of toxicological risk assessment principles to the chemical constituents of cigarette smoke. *Tob. Control* **2003**, *12*, 424–430.
- (9) Hecht, S. S. Tobacco smoke carcinogens and lung cancer. *J. Natl. Cancer Inst.* **1999**, *91*, 1194–1210.
- (10) Behar, R. Z.; Davis, B.; Wang, Y.; Bahl, V.; Lin, S.; Talbot, P. Identification of toxicants in cinnamon-flavored electronic cigarette refill fluids. *Toxicol. In Vitro* **2014**, *28*, 198–208.
- (11) Behar, R. Z.; Luo, W.; Lin, S. C.; Wang, Y.; Valle, J.; Pankow, J. F.; Talbot, P. Distribution, quantification and toxicity of cinnamaldehyde in electronic cigarette refill fluids and aerosols. *Tob. Control* **2016**, *25*, ii94–ii102.
- (12) Goniewicz, M. L.; Knysak, J.; Gawron, M.; Kosmider, L.; Sobczak, A.; Kurek, J.; Prokopowicz, A.; Jablonska-Czapla, M.; Rosik-Dulewska, C.; Havel, C.; Jacob, P., 3rd; Benowitz, N. Levels of selected carcinogens and toxicants in vapour from electronic cigarettes. *Tob. Control* **2014**, *23*, 133–139.
- (13) Schober, W.; Szendrei, K.; Matzen, W.; Osiander-Fuchs, H.; Heitmann, D.; Schettgen, T.; Jörres, R. A.; Fromme, H. Use of electronic cigarettes (e-cigarettes) impairs indoor air quality and increases FeNO levels of e-cigarette consumers. *Int. J. Hyg. Environ. Health* **2014**, *217*, 628–637.
- (14) Kosmider, L.; Sobczak, A.; Fik, M.; Knysak, J.; Zaciera, M.; Kurek, J.; Goniewicz, M. L. Carbonyl compounds in electronic cigarette vapors: effects of nicotine solvent and battery output voltage. *Nicotine Tob. Res.* **2014**, *16*, 1319–1326.
- (15) Zhao, J.; Nelson, J.; Dada, O.; Pyrgiotakis, G.; Kavouras, I. G.; Demokritou, P. Assessing electronic cigarette emissions: linking physico-chemical properties to product brand, e-liquid flavoring additives, operational voltage and user puffing patterns. *Inhalation Toxicol.* **2018**, *30*, 78–88.
- (16) Alderman, S. L.; Song, C.; Moldoveanu, S. C.; Cole, S. K. Particle size distribution of e-cigarette aerosols and the relationship to Cambridge filter pad collection efficiency. *Contrib. Tob. Res.* **2015**, *26*, 183–190.
- (17) Smith, P. H.; Akpara, E.; Haq, R.; El-Miniawi, M.; Thompson, A. B. Gender and menthol cigarette use in the United States: A systematic review of the recent literature (2011 - May 2017). *Curr. Addict. Rep.* **2017**, *4*, 431–438.
- (18) Hersey, J.; Wen Ng, S.; Nonnemaker, J.; Mowery, P.; Thomas, K.; Vilsaint, M. C.; Allen, J.; Lyndon Haviland, M. Are menthol cigarettes a starter product for youth? *Nicotine Tob. Res.* **2006**, *8*, 403–413.
- (19) Glantz, S. A.; Gardiner, P. Local movement to ban menthol tobacco products as a result of federal inaction. *JAMA Intern. Med.* **2018**, *178*, 711–713.
- (20) Pellegrino, R. M.; Tinghino, B.; Mangiaracina, G.; Marani, A.; Vitali, M.; Protano, C.; Osborn, J. F.; Cattaruzza, M. S. Electronic cigarettes: an evaluation of exposure to chemicals and fine particulate matter (PM). *Ann. Ig.* **2012**, *24*, 279–288.
- (21) Schripp, T.; Markewitz, D.; Uhde, E.; Salthammer, T. Does e-cigarette consumption cause passive vaping? *Indoor Air* **2013**, *23*, 25–31.
- (22) Wieslander, G.; Norback, D.; Lindgren, T. Experimental exposure to propylene glycol mist in aviation emergency training: acute ocular and respiratory effects. *Occup. Environ. Med.* **2001**, *58*, 649–655.
- (23) Ohta, K.; Uchiyama, S.; Inaba, Y.; Nakagome, H.; Kunugita, N. Determination of carbonyl compounds generated from the electronic cigarette using coupled silica cartridges impregnated with hydroquinone and 2, 4-dinitrophenylhydrazine. *Bunseki Kagaku* **2011**, *60*, 791–797.
- (24) Bekki, K.; Uchiyama, S.; Ohta, K.; Inaba, Y.; Nakagome, H.; Kunugita, N. Carbonyl compounds generated from electronic cigarettes. *Int. J. Environ. Res. Public Health* **2014**, *11*, 11192–11200.
- (25) Geiss, O.; Bianchi, I.; Barrero-Moreno, J. Correlation of volatile carbonyl yields emitted by e-cigarettes with the temperature of the heating coil and the perceived sensorial quality of the generated vapours. *Int. J. Hyg. Environ. Health* **2016**, *219*, 268–277.
- (26) Wang, P.; Chen, W.; Liao, J.; Matsuo, T.; Ito, K.; Fowles, J.; Shusterman, D.; Mendell, M.; Kumagai, K. A device-independent evaluation of carbonyl emissions from heated electronic cigarette solvents. *PLoS One* **2017**, *12*, No. e0169811.
- (27) U.S. Environmental Protection Agency (EPA). IRIS Toxicological Review of Acrolein (2003 Final). <https://cfpub.epa.gov/ncea/risk/recordisplay.cfm?deid=51977> (accessed Mar 12, 2018).
- (28) Bein, K.; Leikauf, G. D. Acrolein—a pulmonary hazard. *Mol. Nutr. Food Res.* **2011**, *55*, 1342–1360.
- (29) Moretto, N.; Volpi, G.; Pastore, F.; Facchinetti, F. Acrolein effects in pulmonary cells: relevance to chronic obstructive pulmonary disease. *Ann. N.Y. Acad. Sci.* **2012**, *1259*, 39–46.
- (30) Vardavas, C. I.; Anagnostopoulos, N.; Kougiyas, M.; Evangelopoulou, V.; Connolly, G. N.; Behrakis, P. K. Short-term pulmonary effects of using an electronic cigarette: impact on

respiratory flow resistance, impedance, and exhaled nitric oxide. *Chest* **2012**, *141*, 1400–1406.

(31) Pisinger, C.; Dossing, M. A systematic review of health effects of electronic cigarettes. *Prev. Med.* **2014**, *69*, 248–260.

(32) Hua, M.; Talbot, P. Potential health effects of electronic cigarettes: a systematic review of case reports. *Prev. Med. Rep.* **2016**, *4*, 169–178.

(33) U.S. Environmental Protection Agency (EPA). Acrolein. https://cfpub.epa.gov/ncea/iris2/chemicalLanding.cfm?substance_nmbr=364 (accessed May 12, 2019).

(34) The International Agency for Research on Cancer IARC monographs on the evaluation of carcinogenic risks to humans: Chemical agents and related occupations. <https://monographs.iarc.fr/iarc-monographs-on-the-evaluation-of-carcinogenic-risks-to-humans-16/> (accessed May 15, 2019).

(35) U.S. Environmental Protection Agency (EPA). Benzene. https://cfpub.epa.gov/ncea/iris2/chemicalLanding.cfm?substance_nmbr=276 (accessed May 12, 2019).

(36) Varlet, V.; Farsalinos, K.; Augsburger, M.; Thomas, A.; Etter, J.-F. Toxicity assessment of refill liquids for electronic cigarettes. *Int. J. Environ. Res. Public Health* **2015**, *12*, 4796–4815.

(37) Bühler, W.; Dinjus, E.; Ederer, H. J.; Kruse, A.; Mas, C. Ionic reactions and pyrolysis of glycerol as competing reaction pathways in near-and supercritical water. *J. Supercrit. Fluids* **2002**, *22*, 37–53.

(38) Jensen, R. P.; Strongin, R. M.; Peyton, D. H. Solvent chemistry in the electronic cigarette reaction vessel. *Sci. Rep.* **2017**, *7*, 42549.

(39) Strongin, R. M. E-Cigarette chemistry and analytical detection. *Annu. Rev. Anal. Chem.* **2019**, *12*, 23–39.

(40) El-Hellani, A.; Salman, R.; El-Hage, R.; Talih, S.; Malek, N.; Baalbaki, R.; Karaoghanian, N.; Nakkash, R.; Shihadeh, A.; Saliba, N. A. Nicotine and carbonyl emissions from popular electronic cigarette products: correlation to liquid composition and design characteristics. *Nicotine Tob. Res.* **2018**, *20*, 215–223.

(41) El-Hellani, A.; Al-Moussawi, S.; El-Hage, R.; Talih, S.; Salman, R.; Shihadeh, A.; Saliba, N. A. Carbon monoxide and small hydrocarbon emissions from sub-ohm electronic cigarettes. *Chem. Res. Toxicol.* **2019**, *32*, 312–317.

(42) Uchiyama, S.; Ohta, K.; Inaba, Y.; Kunugita, N. Determination of carbonyl compounds generated from the E-cigarette using coupled silica cartridges impregnated with hydroquinone and 2, 4-dinitrophenylhydrazine, followed by high-performance liquid chromatography. *Anal. Sci.* **2013**, *29*, 1219–1222.

(43) Herrington, J. S.; Myers, C. Electronic cigarette solutions and resultant aerosol profiles. *J. Chromatogr. A* **2015**, *1418*, 192–199.

(44) Gil-Av, E.; Shabtai, J.; Steckel, F. Thermal aromatization of 1, 3-Butadiene. *Ind. Eng. Chem.* **1960**, *52*, 31–32.

(45) Dagaut, P.; Cathonnet, M. The oxidation of 1, 3-butadiene: Experimental results and kinetic modeling. *Combust. Sci. Technol.* **1998**, *140*, 225–257.

(46) Jones, B. M.; Zhang, F.; Kaiser, R. I.; Jamal, A.; Mebel, A. M.; Cordiner, M. A.; Charnley, S. B. Formation of benzene in the interstellar medium. *Proc. Natl. Acad. Sci. U.S.A.* **2011**, *108*, 452–457.

(47) Pankow, J. F.; Kim, K.; McWhirter, K. J.; Luo, W.; Escobedo, J. O.; Strongin, R. M.; Duell, A. K.; Peyton, D. H. Benzene formation in electronic cigarettes. *PLoS One* **2017**, *12*, No. e0173055.

(48) Poklis, J. L.; Wolf, C. E.; Peace, M. R. Ethanol concentration in 56 refillable electronic cigarettes liquid formulations determined by headspace gas chromatography with flame ionization detector (HS-GC-FID). *Drug Test. Anal.* **2017**, *9*, 1637–1640.

(49) MistHub. Significance of variable voltage and vaping power chart, 2013. <https://www.misthub.com/blogs/vape-tutorials/76788421-tutorial-variable-voltage-and-vaping-power-chart> (accessed June 21, 2019).

(50) Geiss, O.; Bianchi, I.; Barrero-Moreno, J. Correlation of volatile carbonyl yields emitted by e-cigarettes with the temperature of the heating coil and the perceived sensorial quality of the generated vapours. *Int. J. Hyg. Environ. Health* **2016**, *219*, 268–277.

(51) Talih, S.; Balhas, Z.; Salman, R.; Karaoghanian, N.; Shihadeh, A. “Direct dripping”: a high-temperature, high-formaldehyde emission electronic cigarette use method. *Nicotine Tob. Res.* **2016**, *18*, 453–459.

(52) Ogunwale, M. A.; Li, M.; Ramakrishnam Raju, M. V.; Chen, Y.; Nantz, M. H.; Conklin, D. J.; Fu, X.-A. Aldehyde detection in electronic cigarette aerosols. *ACS Omega* **2017**, *2*, 1207–1214.

(53) Davis, J. L.; Barteau, M. A. Polymerization and decarbonylation reactions of aldehydes on the Pd (111) surface. *J. Am. Chem. Soc.* **1989**, *111*, 1782–1792.

(54) Tena, A. F.; Clarà, P. C. Deposition of inhaled particles in the lungs. *Arch. Bronconeumol.* **2012**, *48*, 240–246.

(55) Sosnowski, T. R.; Odziomek, M. Particle size dynamics: Toward a better understanding of electronic cigarette aerosol interactions with the respiratory system. *Front. Physiol.* **2018**, *9*, 853.

(56) Biswas, P.; Jones, C. L.; Flagan, R. C. Distortion of size distributions by condensation and evaporation in aerosol instruments. *Aerosol Sci. Technol.* **1987**, *7*, 231–246.

(57) Margham, J.; McAdam, K.; Forster, M.; Liu, C.; Wright, C.; Mariner, D.; Proctor, C. Chemical composition of aerosol from an e-cigarette: a quantitative comparison with cigarette smoke. *Chem. Res. Toxicol.* **2016**, *29*, 1662–1678.

(58) Beauval, N.; Antherieu, S.; Soyez, M.; Gengler, N.; Grova, N.; Howsam, M.; Hardy, E. M.; Fischer, M.; Appenzeller, B. M. R.; Goossens, J.-F.; Allorge, D.; Garçon, G.; Lo-Guidice, J.-M.; Garat, A. Chemical evaluation of electronic cigarettes: Multicomponent analysis of liquid refills and their corresponding aerosols. *J. Anal. Toxicol.* **2017**, *41*, 670–678.

(59) Chung, S.-S.; Zheng, J.-S.; Kwong, A. C. S.; Lai, V. W. Y. Harmful flame retardant found in electronic cigarette aerosol. *J. Cleaner Prod.* **2018**, *171*, 10–16.

(60) Keum, Y.-S.; Li, Q. X. Reductive debromination of polybrominated diphenyl ethers by zerovalent iron. *Environ. Sci. Technol.* **2005**, *39*, 2280–2286.

(61) Yerger, V. B. Menthol’s potential effects on nicotine dependence: a tobacco industry perspective. *Tob. Control* **2011**, *20*, ii29–ii36.

(62) Soulet, S.; Duquesne, M.; Toutain, J.; Pairaud, C.; Lalo, H. Influence of Coil Power Ranges on the E-Liquid Consumption in Vaping Devices. *Int. J. Environ. Res. Public Health* **2018**, *15*, 1853.

(63) Korzun, T.; Lazurko, M.; Munhenzva, I.; Barsanti, K. C.; Huang, Y.; Jensen, R. P.; Escobedo, J. O.; Luo, W.; Peyton, D. H.; Strongin, R. M. E-cigarette airflow rate modulates toxicant profiles and can lead to concerning levels of solvent consumption. *ACS Omega* **2018**, *3*, 30–36.

(64) Jasinska, A. J.; Zorick, T.; Brody, A. L.; Stein, E. A. Dual role of nicotine in addiction and cognition: a review of neuroimaging studies in humans. *Neuropharmacology* **2014**, *84*, 111–122.

(65) Pagano, T.; DiFrancesco, A. G.; Smith, S. B.; George, J.; Wink, G.; Rahman, I.; Robinson, R. J. Determination of nicotine content and delivery in disposable electronic cigarettes available in the United States by gas chromatography-mass spectrometry. *Nicotine Tob. Res.* **2016**, *18*, 700–707.

(66) Buettner-Schmidt, K.; Miller, D. R.; Balasubramanian, N. Electronic cigarette refill liquids: child-resistant packaging, nicotine content, and sales to minors. *J. Pediatr. Nurs.* **2016**, *31*, 373–379.

(67) Kim, S.; Goniewicz, M.; Yu, S.; Kim, B.; Gupta, R. Variations in label information and nicotine levels in electronic cigarette refill liquids in South Korea: regulation challenges. *Int. J. Environ. Res. Public Health* **2015**, *12*, 4859–4868.